Amino Acids (2021) 53:609–619
https://doi.org/10.1007/s00726-021-02964-2

ORIGINAL ARTICLE

Interaction of cationic surfactants with DPPC membranes: effect of a novel N^{α}-benzoylated arginine-based compound

Melisa Hermet[1,5] · M. Elisa Fait[1,5] · Romina F. Vazquez[2,5,6] · Sabina Mate[2,5] · M. Antonieta Daza Millone[3,5] · M. Elena Vela[3] · María Teresa García[4] · Susana R. Morcelle[1,5] · Laura Bakas[1]

Received: 2 December 2020 / Accepted: 19 February 2021 / Published online: 12 March 2021
© The Author(s), under exclusive licence to Springer-Verlag GmbH, AT part of Springer Nature 2021

Abstract

Cationic amino acid-based surfactants are known to interact with the lipid bilayer of microorganism resulting in cell death through a disruption of the membrane topology. To elucidate the interaction of a cationic surfactant synthesized in our lab, investigations involving N^{α}-benzoyl-arginine decyl amide (Bz-Arg-NHC_{10}), and model membranes composed by 1,2-dipalmitoyl-*sn*-glycero-3-phosphocholine (DPPC) were done. Bz-Arg-$NHC_{10}$was able to penetrate into DPPC monolayers up to a critical pressure of 59.6 mN m^{-1}. Differential scanning calorimetry revealed that as the concentration of Bz-Arg-NHC_{10} increased, the main transition temperature of DPPC slightly decreased. Atomic force microscopy (AFM) in situ experiments performed on supported DPPC bilayers on mica allowed monitoring the changes induced by Bz-Arg-NHC_{10}. DPPC bilayer patches were partially removed, mainly in borders and bilayer defects for 50 μM Bz-Arg-NHC_{10} solution. Increasing the concentration to 100 μM resulted in a complete depletion of the supported bilayers. Surface plasmon resonance (SPR) experiments, carried out with fully DPPC bilayers covered chips, showed a net increase of the SPR signal, which can be explained by Bz-Arg-NHC_{10} adsorption. When patchy DPPC bilayers were formed on the substrate, a SPR signal net decrease was obtained, which is consistent with the phospholipids' removal observed in the AFM images. The results obtained suggest that the presence of the benzoyl group attached to the polar head of our compound would be the responsible of the increased antimicrobial activity against gram-negative bacteria when compared with other arginine-based surfactants.

Keywords Arginine-based surfactants · Model biological membranes · DPPC bilayer · Antibacterial activity

Introduction

The use of surfactants is widely spread in everyday life, since they are ingredients of many formulations, ranging from cleansing agents for household and personal care to emulsifiers and preservatives in food and pharmaceutical preparations. The reason for this is based on their biological and physicochemical properties, which are given by their amphiphilic nature. Due to the paramount importance of these compounds, which are manufactured and consumed at worldwide scale, the development of new products with low

Handling editor: J. G. López.

✉ Susana R. Morcelle
morcelle@biol.unlp.edu.ar

✉ Laura Bakas
lbakas@biol.unlp.edu.ar

[1] Centro de Investigación de Proteínas Vegetales (CIProVe), Departamento de CienciasBiológicas, Facultad de Ciencias Exactas, Universidad Nacional de La Plata (UNLP), Centro Asociado CICPBA, La Plata, Buenos Aires, Argentina

[2] Instituto de Investigaciones Bioquímicas La Plata (INIBIOLP), CCT-La Plata, CONICET, Facultad de Ciencias Médicas, Universidad Nacional de La Plata, La Plata, Buenos Aires, Argentina

[3] Instituto de Investigaciones Fisicoquímicas Teóricas y Aplicadas (INIFTA), CCT-La Plata, CONICET, Universidad Nacional de La Plata, La Plata, Buenos Aires, Argentina

[4] Departamento de Tensioactivos y Nanotecnología, IQAC-CSIC, Barcelona, Spain

[5] Centro Científico Tecnológico del Consejo Nacional de Investigaciones Científicas (CONICET, CCT-La Plata), La Plata, Argentina

[6] Departamento de Química, Facultad de Ciencias Exactas, Universidad Nacional de La Plata, 47 y 115, 1900 La Plata, Argentina

environmental impact and minimal toxicity is mandatory. Within this context, amino acid-based surfactants represent an attractive alternative to the more conventional ones, since they resemble natural amphiphilic molecules and can be obtained from renewable raw materials (Pinazo et al. 2011). Furthermore, the chemical groups that amino acids possess allow the possibility of attaching different acyl/alkyl chains by amide, ester or alkyl linkage, generating a great variety of structures with diverse properties (Tripathy et al. 2018). These compounds have some characteristics in common, such as minimal toxicity and low irritancy, high biodegradability and good antimicrobial activity, being the most studied those arginine-based ones (Pinazo et al. 2019). Arginine-based surfactants can be obtained by sustainable methods such as biocatalytic strategies, and have low toxicity profile, high biodegradability and exceptional antimicrobial properties due to the presence of both the guanidine group of the arginine residue and the alkyl chain length (Infante et al. 1985, 1997; Morán et al. 2004).

The antimicrobial action of cationic surfactants is supposed to be based on their ability to disrupt the microbial membrane through a combined adsorption and hydrophobic phenomenon at the membrane/water interface followed by membrane disorganization (Castillo et al. 2006). In this regard, the cationic surfactants are strongly adsorbed on the bacterial cell surface due to the presence of ionic charges in the molecule, triggering membrane disruption. Morán et al. (2001) published results showing that arginine *O*-alkyl amides (C_{10}–C_{14}) and arginine *O*-alkyl esters (C_8–C_{12}) with two positive charges per head group showed the lowest MIC values (Morán et al. 2001). On the other hand, Colomer and coworkers proved that the addition of a lysine residue as a second amino acid in the polar portion of the molecule reduced biocidal activity due to the presence of two cationic charges, which increased the hydrophilic character of the molecule and, consequently, reduced the surface activity (Colomer et al. 2011).

Regarding the length of the hydrophobic chain, for the three monocatenary surfactant series, N^{α}-alkyl amides, O^{α}-alkyl amides, and O^{α}-alkyl esters, the highest antimicrobial effect was observed for those compounds with 12-carbon alkyl chains (Morán et al. 2001). This fact was attributed to the combination of several physicochemical properties, such as hydrophobicity, adsorption strength, CMC, and solubility in aqueous media. However, it is important to point out that the optimum alkyl chain length depends on the surfactant structure.

Our group has previously synthesized and characterized some arginine-based surfactants using an endopeptidase from *Carica papaya* latex—papain—as biocatalyst and a purification methodology based on ecofriendly techniques (Fait et al. 2015). Among the compounds synthesized within this family of surfactants, N^{α}-benzoyl-arginine decylamidehydrochloride (Bz-Arg-NHC_{10}) demonstrated an interesting potential for its use as a disinfectant, due to the antimicrobial activity showed against both gram-positive and gram-negative bacteria and fungi. Besides, it proved to have lower toxicity and irritancy when compared with other commercial tensioactives of cationic nature. These properties turn Bz-Arg-NHC_{10} into a promising candidate for its application in topical formulations as a preservative agent or as an antiseptic itself.

The present work examines the physicochemical process involved in the perturbation of the lipidmembrane induced by Bz-Arg-NHC_{10}, schematically represented in Fig. 1. To this end, the interaction of this surfactant with different biomembrane models, namely, 1,2-dipalmitoyl *sn*-glycero-3-phosphocholine (DPPC) multilamellar lipid vesicles (MLVs), monolayers and supported bilayers was evaluated using different experimental approaches, including Langmuir monolayer, differential scanning calorimetry analysis (DSC), atomic force microscopy (AFM) and surface plasmon resonance (SPR).

Materials and methods

Chemicals

1,2-Dipalmitoyl-sn-glycero-3-phosphocholine (DPPC), DL-dithiothreitol (DTT), *N*-(2-hydroxyethyl)piperazine-*N*′-(2-ethanesulfonic acid) (HEPES) and other reagents, all analytical-grade, were purchased from Sigma Aldrich (USA) and Tris base and methanol HPLC-grade from J. T. Baker (USA). The arginine-based cationic surfactant Bz-Arg-NHC_{10}·HCl was synthesized as previously described using papain adsorbed onto polyamide as biocatalyst (Fait et al. 2015). For all the solutions and experiments ultrapure MilliQ (Merck Millipore, USA) water was used, and had a resistivity of 18.2 MΩ cm^{-1}. Gold evaporated (~ 50 nm) on glass substrates (SPR102-AU) were obtained from Bionavis (Finland). Muscovite mica grade V-1 was

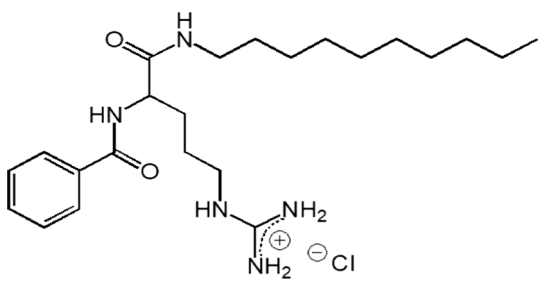

Fig. 1 N^{α}-Benzoyl-arginine decylamide (Bz-Arg-NHC_{10}) chemical formula

purchased from SPI Supplies (USA). The rest of the chemicals used in this work were of analytical grade.

Critical micelle concentration (CMC)

The surface tension measurements at equilibrium were performed with a Krüss K12 tensiometer (Hamburg, Germany) by means of the Wilhelmy plate method. A stock solution of the surfactant (0.335 mM) was prepared in phosphate buffered saline (PBS) pH 7.4 (6.78 g L^{-1} NaCl, 1.42 g L^{-1} Na_2HPO_4 and 0.4 g L^{-1} KH_2PO_4 in MilliQ water). The experiment was performed in an appropriate glass cell containing PBS at the beginning of the assay. For the CMC estimation, the surface tension of a solution of increasing concentration of Bz-Arg-NHC_{10}·HCl was measured after each addition of a small volume of the stock solution and the subsequent 15–20 min equilibration at 25 °C. The CMC was estimated from the intersection between the two linear portions of the γ vs. log C plot.

Preparation of DPPC MLVs and SUVs suspensions

Multilamellar vesicles (MLVs) of DPPC used for the DSC assays were obtained as follows. A standard solution of DPPC (3.33 mg mL^{-1}) in $CHCl_3$/MeOH 1:1 V V^{-1} was prepared and aliquoted (100 µL) in glass test tubes. The solvent was removed under a nitrogen stream while rotating the tube to form a thin film of lipid and left under reduced pressure for at least 2 h to eliminate all traces of solvent. MLVs were obtained by hydrating the lipid film with 100 µL of PBS, containing the corresponding amount of surfactant (from 0 to 4 mol%), followed by five alternative cycles of vortex and heating at 60 °C (2 min). To assure a significant interaction between the surfactant and the liposomal structures, the final solutions were left overnight.

For AFM and SPR measurements, DPPC MLVs were prepared by addition of buffer HEPES (25 mM HEPES, 150 mM NaCl pH 7.4) or TBS (20 mM Tris base, 150 mM NaCl pH 7.4), respectively, to the thin lipid film, followed by vigorous vortexing at 60 °C. In both cases, the MLVs suspensions were sonicated at 60 °C for 1 h using a TestLab TB04 bath-type sonicator (Buenos Aires, Argentina). Hence, small unilamellar vesicles (SUV) were generated.

SUVs where characterized by means of DLS with a Malvern Zetasizer Nano (Malvern Instruments, UK) equipped with a laser (633 nm) set at angle of 173°. Measurements made in PBS buffer at 25 °C gave a mean size of 85 ± 6 nm (PDI = 0.18 ± 0.02).

Differential scanning calorimetry (DSC)

Differential scanning calorimetry measurements of DPPC MLVs were carried out in a DSC Q100 TA Instruments (USA) calorimeter at a scanning rate of 5 °C min^{-1}. Aluminum pans were loaded with MLV suspension (0.2 mg of DPPC) and submitted to heating/cooling cycles between 0 and 60 °C. At least two runs were performed for each sample. The data from the first run were always discarded. Experiments were carried out in duplicate. Data analysis was done using the TA Universal Analysis software.

Monolayer penetration experiments

Surface-pressure (π) measurements were carried out with a Langmuir trough by a NIMA Model 102A instrument (NIMA Technology, Coventry, UK) with a Wilhelmy plate as the π sensor. The aqueous subphase consisted of PBS buffer prepared in ultrapure Milli-Q water. For monolayer penetration assays, DPPC monolayers were formed by spreading the lipids from a stock solution prepared in chloroform (1 mM) over the subphase surface until the desired initial surface pressure (π_o) of the lipid film was attained. After waiting 15 min for complete solvent evaporation and π_o stabilization, the measurement was started, and the surface pressure of the neat lipid monolayer was recorded. Then, Bz-Arg-NHC_{10} from a stock solution prepared in PBS was injected into the subphase bulk with a Hamilton microsyringe to reach a final concentration of 30 µM and the increment in π ($\Delta\pi$) was recorded over time until a stable signal was obtained. Measurements were performed at 23 ± 1 °C.

Atomic-force microscopy (AFM)

Ex-situ lipid samples were prepared in freshly cleaved planchets of mica. First, a 5 µL drop of 1 mM $CaCl_2$ was added to the mica and after 15 min, the surface was washed with MilliQ water. Then, 100 µL of DPPC SUVs were dropped on the Ca^{2+} modified mica and allowed to interact for 1 h at 60 °C. The unbounded lipid vesicles were washed with buffer solution. Samples were placed without drying in the AFM fluid chamber, and then filled with 50 µL of HEPES buffer. After scanning the surface, an aliquot (30 µL) of surfactant solution was added and the changes induced by the addition of Bz-Arg-NHC_{10} were followed during time (10–20 min). To assess that these observations were not due to invasive AFM tip interaction with the membrane, consecutive scans of the same area without surfactant were also recorded.

AFM measurements were performed on a MultiMode Scanning Probe Microscope controlled by a Nanoscope-V unit (Veeco Instruments Inc., USA) using V-shaped Si_3N_4 probes (Veeco Instruments Inc., USA) with 0.08–0.15 N m^{-1} spring constants. All the experiments

were carried out at 24 °C in a fluid cell. Images were obtained in contact mode with a scanning rate of 1 Hz.

Surface plasmon resonance (SPR) measurements

SPR measurements were performed in MP-SPR Navi™200 (BioNavis, Finland) equipped with two independent lasers (670 and 785 nm) in a dual-channel detection system. Measurements were made in an angular-scan range of 58–72 degrees and typical flows employed were 10–500 µL min^{-1}.

Preparation of the sensor surfaces

Commercial gold substrates (SPR102-AU, Bionavis) were washed with NH_3:H_2O_2:H_2O (1:1:2) at 90 °C during 10 min, rinsed with water and ethanol and dried with N_2. Immediately, the substrates were incubated in the presence of a 50 µM DTT ethanolic solution for 30 min at room temperature. The DTT-gold substrates were thoroughly rinsed with ethanol and dried with N_2.

Liposome binding

DPPC SUVs were employed for the in situ generation of lipid bilayers on the surface of the SPR sensor chip. DTT-gold substrates were placed in the SPR device and the SPR curves (from 58 to 72 degrees) were registered each 3 s. The running buffer was TBS with 3 mM Ca^{2+} kept at a flow of 10 µL min^{-1} for all the experiments. After 10 min of baseline stabilization, the 0.2 mg mL^{-1} liposome suspension was injected at 10 µL min^{-1} during 15 min, with one or more steps for different surface coverages, in both flow cells. After 10 min of stabilization, a quick pulse of running buffer at 500 µL min^{-1} was performed to remove weakly adsorbed material. The amount of bound lipid was calculated from the change in the signal registered at the angle of maximum derivative ($\Delta\Theta_{bilayer}$) from the initial baseline and the signal after the washing step. Results were expressed as the percentage of the theoretical $\Delta\Theta_{bilayer}$ expected for a full bilayer coverage (Daza Millone et al. 2018).

Surfactant affinity measurements

After supported bilayer preparation, surfactant solutions prepared in TBS buffer were injected at 10 µL min^{-1} during 30 min through the main channel, while buffer (TBS) was injected in the control channel. Duplicate measurements were performed for each sample using freshly prepared supported bilayers. Also, control experiments were made injecting the surfactant solutions on DTT surfaces, i.e., without the DPPC bilayer.

Results

Cationic lipoamino acids constitute an important class of natural surface-active biomolecules of great interest to organic and physical chemists and to biologists with an unpredictable number of basic and industrial applications (Pinazo et al. 2019). Among others, antimicrobial activity is one of the most remarkable biological properties of this kind of compounds (Fait et al. 2019). This fact is attributed to the combination of several physicochemical parameters—such as the CMC, the surfactant's hydrophobicity, the adsorption strength, and water solubility, among others—which results in an optimal hydrophobic/hydrophilic balance that enhance the interaction and penetration of the surfactant into the microorganism's membrane. In all instances, both the alkyl chain length and the chemistry of the polar head group affect the biocidal activity. Within this context, the physicochemical parameters of Bz-Arg-NHC_{10} and its interaction with model membranes were studied.

Physicochemical characterization

Basic physicochemical parameters that characterize a surface-active compound are CMC, surface tension at the CMC (γ_{CMC}), the maximum surface excess concentration at the air/aqueous solution interface (Γ_{max}), and the area per molecule (A_{min})—which measures the minimum area per surfactant molecule at air/aqueous solution interface. The CMC and γ_{CMC} can be determined from the break point of the surface tension (γ) vs. the logarithm of the surfactant concentration curves. And using the Gibbs adsorption equation, we can also obtain both Γ_{max} and A_{min} (Rosen 2004). All parameters are summarized in Table 1.

Several studies have reported adsorption and self-aggregation in aqueous media at a range of concentrations and in either the presence or the absence of other components for single chain arginine-based surfactants (Pinazo et al. 2011). We previously demonstrated the surfactant character of Bz-Arg-NHC_{10} in aqueous media, proving its ability to reduce the surface tension of water (Fait et al. 2017). Within this context, self-aggregation was also evidenced, showing a defined CMC value of 0.230 mM at 25 °C. Since the presence of salts in the medium (buffer solution) used in the experiments modifies

Table 1 Bz-Arg-NHC_{10} surface parameters in PBS

Medium	CMC (mM)	γ_{CMC} (mN m^{-1})	Π_{CMC} (mN m^{-1})	Γ_{max} (10^{10} mol cm^{-2})	A_{min} (Å^2)
PBS	0.028	36.7	35.3	2.47	67

the aggregation properties of the surfactant, the determination of the CMC of Bz-Arg-NHC_{10} in PBS was performed. The selection of PBS was based on the fact that a stock solution of the surfactant in this medium was used for both the monolayers penetration assays and the preparation of DPPC MLVs for the DSC studies (see "Materials and Methods" section). As expected, the CMC obtained in this saline medium was lower than in deionized water (0.028 and 0.230 mM, respectively, Fait et al. 2017). The effect of salts on the micellization of this kind of compounds reveals that in general the CMC values become lower as the concentration of salts in the medium increases.

Critical micelle concentration (CMC), surface tension at CMC (γ_{CMC}), effectiveness of surface tension reduction (Π_{CMC}), maximum adsorption at the interface liquid–air (Γ_{max}) and minimum area occupied by adsorbed molecule at the interface liquid–air (A_{min}).

Interaction of Bz-Arg-NHC_{10} with model membranes

Even though for most bacteria the main zwitterionic phospholipid is phosphatidylethanolamine (PE), we used monolayers, liposomes and supported bilayers composed of DPPC as lipid models to elucidate the antimicrobial mechanism of Bz-Arg-NHC_{10}. This choice was made on the basis of the advantages these systems offer over more complex lipid mixtures (Epand and Epand 2009; Lind et al. 2019), although these will be necessary in order to identify specific interactions between the surfactant and a particular component of the bacterial membrane (Castillo et al. 2004; Colomer et al. 2013). Within this context, differential scanning calorimetry (DSC), Langmuir monolayers, atomic force microscopy (AFM), and surface plasmon resonance (SPR) studies will serve as an initial approach to give an insight into the interaction of this kind of compounds and bacterial membranes.

Differential scanning calorimetry (DSC)

DSC is a tool for assessing the thermodynamic properties of a system, specifically allowing the inspection of a phase transition phenomenon. Heat capacity profiles measure this property as function of the temperature at constant pressure. The presence of peaks in these profiles indicates phase transitions. Surfactants, due to their amphiphilic structure, can be incorporated into the lipid barrier and thus disrupt the tight arrangement of the membrane lipids, inducing a phase transition that can be registered using this technique.

In this work, DSC allowed us to study the effect of Bz-Arg-NHC_{10} on DPPC bilayers. By these means, two parameters were studied. On one hand, we analyzed the main phase transition temperature (T_m), which corresponds to the gel–liquid crystalline transition and is related to *gauche* isomerization of the acyl chains. On the other hand, the width at half-height of the heat absorption peak ($\Delta T_{1/2}$) was also determined, which is a measure of the cooperativity of the transition process.

The effect of Bz-Arg-NHC_{10} in a range of concentrations comprised between 0 and 4 mol% on DPPC MLVs is presented by the thermograms depicted in Fig. 2a. In the absence of the surfactant (control curve), the main transition took place at 41.2 °C. Since the amount of compound enclosed in the DSC capsules was not the same for each determination, the enthalpy values could not be directly recovered from the thermograms. A decrease in the lipidic bilayer fluidity due to the incorporation of Bz-Arg-NHC_{10} can be attributed to hydrophobic mismatch (Inoue et al. 1988). Within this context, compounds bearing ten or less carbon alkyl chains would penetrate into the hydrophobic core of the lipid bilayer in such a fashion that avoid near the acyl hydrocarbon core is created, reducing the stability of the lamellar gel phase and lowering T_m. As can be inferred by the broadening of the endothermic peak, the correlation between the lipid molecules in the phase transition, or cooperativity, was disrupted by the presence of Bz-Arg-NHC_{10}. This fact allows us to infer that the compound was incorporated into the DPPC MLVs.

The parameters obtained from Fig. 2b, c were $\Delta T_m = 0.395$ and $\Delta T_{1/2} = 1.64$. From this experiment, it can be concluded that Bz-Arg-NHC_{10} has a slight efficiency in the fluidification of DPPC bilayers in the assayed conditions; higher concentrations of the compound could not be tested since its low aqueous solubility.

Monolayer penetration experiments

The interaction of Bz-Arg-NHC_{10} with DPPC monolayers was investigated by injecting the surfactant solution into the aqueous subphase (30 µM final concentration), beneath the monolayers compressed at different initial surface pressures (π_o) and analyzing the increment in π ($\Delta\pi$) over time. Figure 3a shows representative curves obtained for DPPC monolayers at π_o of 5 and 20 mN m^{-1}. Upon injection, regardless the π_o of the lipid films, the interaction of Bz-Arg-NHC_{10} with the monolayers resulted in a rapid increase in π within the first 5 min. After this initial increment, a progressive decrease in π was detected within the next 5 min, suggesting a reorganization of the monolayer after adsorption/incorporation of Bz-Arg-NHC_{10} molecules. The monolayers finally became stabilized reaching an equilibrium π (π_{eq}). Interestingly, the net decrease from the maximum π (π_{max}) was ~4 mN m^{-1} for all the π_o tested, which could arise from the detergent-like behavior of this compound that once incorporated into the lipid film may reach a surface concentration high enough to induce the removal of lipid molecules

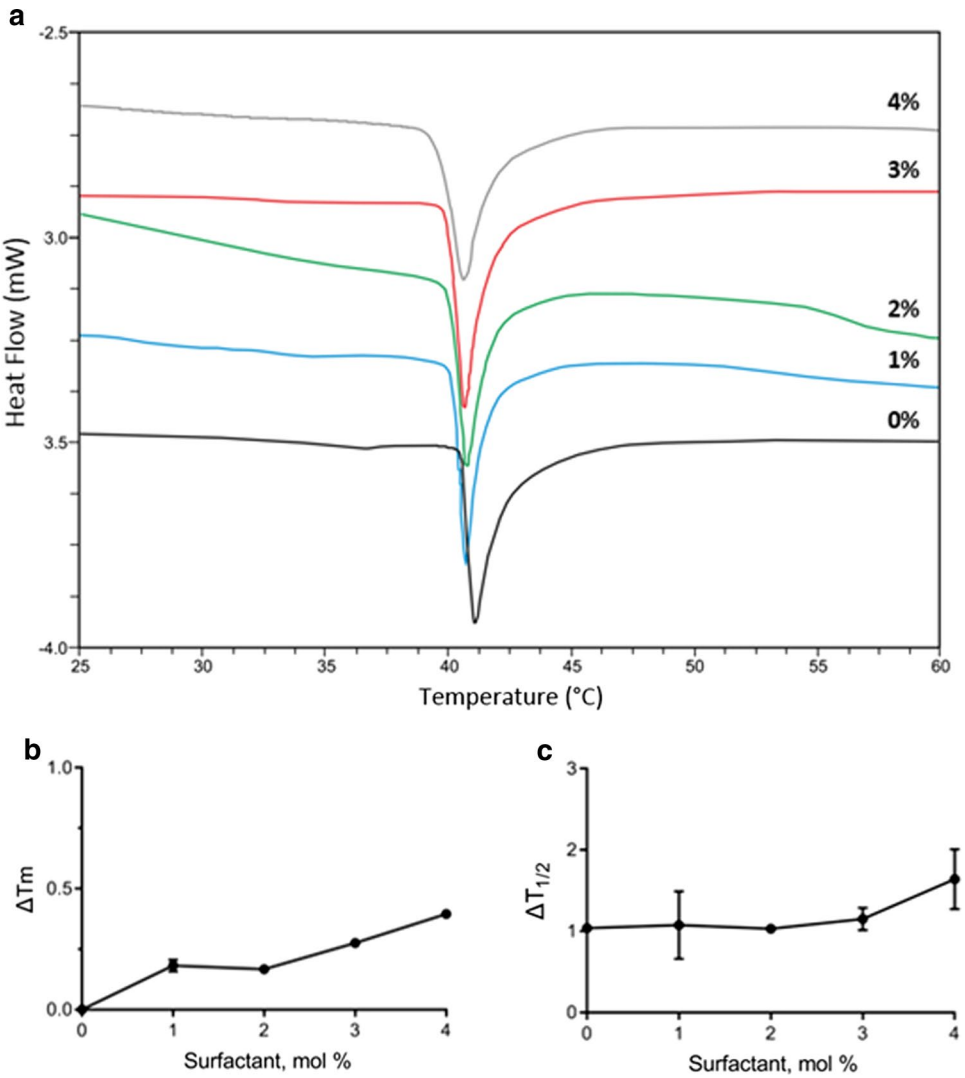

Fig. 2 **a** DSC heating thermograms of DPPC MLVs in the presence of increasing concentrations of Bz-Arg-NHC_{10} (from 0 up to 4 mol%). The heating rate was 5 °C min^{-1}. **b** Depression of the transition temperature ($\Delta T = T_m - T_{m0}$) and **c** the transition width ($\Delta T_{1/2}$) of DPPC MLVsas a function of the molar percentage of surfactant concentrations

from the monolayer to the subphase and the resulting formation of mixed micelles (Nitenberg et al. 2018). For the different π_o assayed, similar kinetics were observed, though the total $\Delta\pi$ (both $\Delta\pi_{max}$ and $\Delta\pi_{eq}$) achieved depended on the π_o value of the lipid film (Fig. 3b)—as the π_o of the monolayer increased, the incorporation of Bz-Arg-NHC_{10} decreased (i.e., a lower $\Delta\pi$ registered) due to the closer packing of the lipids at a higher π_o. From the plot of $\Delta\pi_{max}$ values observed as a function of π_o, the critical surface pressure (π_c) was calculated. This π_c corresponds to the extrapolated value of π_o beyond which no further incorporation of the surfactant into the monolayer would occur (i.e., $\Delta\pi_{max} = 0$ after injection) and reflects the influence of the lipid packing density on the ability of the molecule to penetrate into the monolayer, and hence, its penetration capacity. By these means, the value of π_c obtained was 59.6 mN m^{-1} for Bz-Arg-NHC_{10} in DPPC monolayers.

Atomic force microscopy (AFM)

Biological samples can be observed at the highest resolution under conditions close to their natural state by means of atomic force microscopy (AFM) (Müller et al. 2002). Using this technique, we characterized the interaction of Bz-Arg-$NCH_{10}$with supported lipid membranes. The AFM image (Fig. 4a) showed DPPC bilayers in gel phase, with a thickness of 4.3 ± 0.3 nm as shown in the corresponding cross-section. This difference in the step height with the level of the mica can be considered in the range of values generally observed for supported phospholipid bilayers.

After surfactant's injection in the fluid chamber (50 µM, $t = 0$, Fig. 4b), sequential AFM images of the same area were recorded (Fig. 4b, c). The DPPC supported bilayer height remained unaltered (4.4 ± 0.3 nm) but some holes appeared within it. Besides, most of the bilayer border regions exhibit typical heights of 3.5 ± 0.3 nm. It is not clear what these lower regions are due to, but it has been reported that

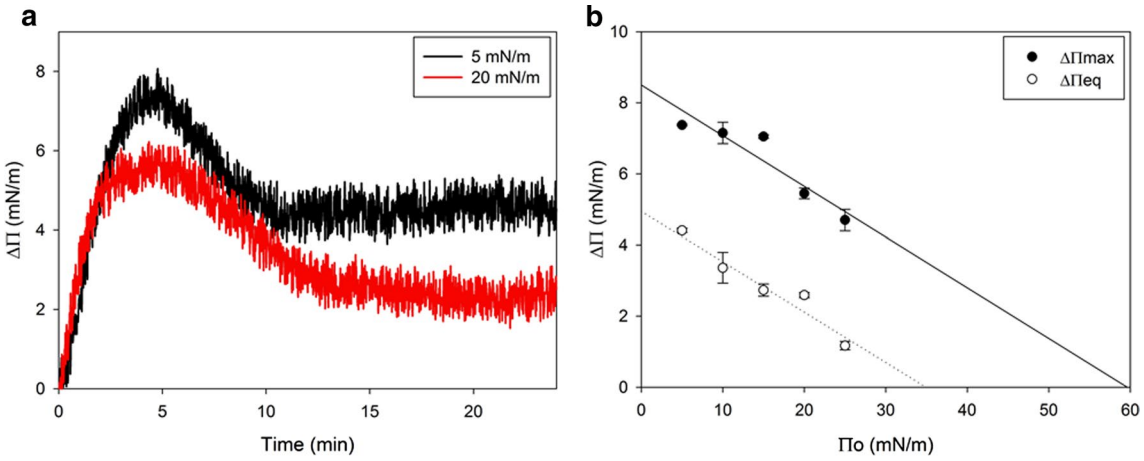

Fig. 3 Bz-Arg-NHC_{10} interaction with DPPC monolayers. **a** Insertion kinetics of Bz-Arg-NHC_{10} into lipid monolayers of DPPC. The lipids were spread over the subphase (PBS buffer) to achieve the initial surface pressures (π_o) indicated in the figure. Bz-Arg-NHC_{10} was then injected from a stock solution in PBS to give a final concentration of 30 μM and the increase in surface pressure ($\Delta\pi$) was registered over time. **b** Maximum and equilibrium $\Delta\pi$ ($\Delta\pi_{max}$ and $\Delta\pi_{eq}$) obtained for the interaction of Bz-Arg-NHC_{10} with DPPC monolayers at different π_o. The critical surface pressure (π_c) was obtained by extrapolating the curve of $\Delta\pi_{max}$ vs. π_o to $\Delta\pi = 0$. The values represent the mean ± SEM, $n = 3$. Measurements were performed at 23 ± 1 °C

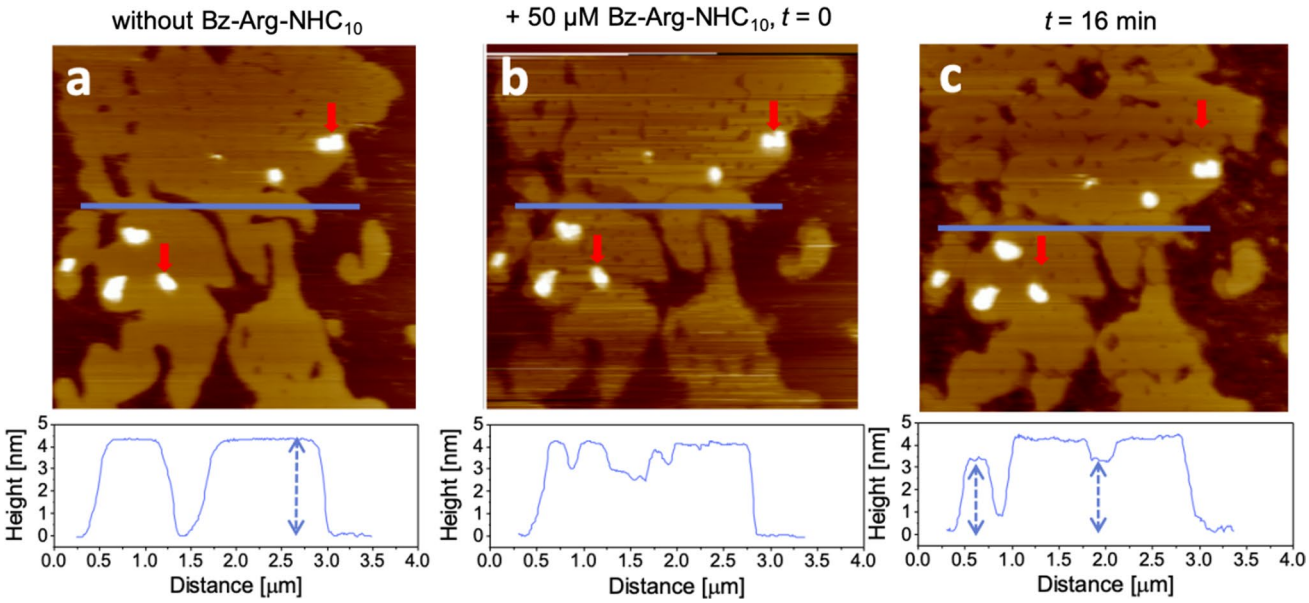

Fig. 4 AFM images of Bz-Arg-NHC_{10} interaction (50 μM) with DPPC supported bilayers. **a** 4 μm × 4 μm image taken before the interaction, **b** immediately after the injection of 50 μM Bz-Arg-NHC_{10}, and **c** at $t = 16$ min (subsequent scans). Cross-sections shown below correspond to the blue lines drawn in the images. Brighter spots are associated to vesicles (red arrows)

surfactants intercalate preferentially in regions where the molecular packing is less dense, i.e., the border of the bilayer (Lima et al. 2013). This intercalation would induce disorder in the DPPC gel phase causing a phase transition from gel to a liquid-crystalline state. Based on different heights measured, it can be presumed that the higher domains are essentially DPPC-rich domains while the lower ones are Bz-Arg-NHC_{10}-rich domains.

For all samples, vesicles that were not removed by surfactant's addition were also observed (red arrows in Fig. 4).

The AFM image (Fig. 5a) showed DPPC bilayers in the gel phase, with a thickness of 4.3 ± 0.3 nm. Furthermore, 16 min after the injection of Bz-Arg-NHC_{10}, re-adsorption of material on the mica surface was observed (Fig. 5b). This could be due to the formation of lipid-surfactant mixed micelles (Morandat and El Kirat 2007).

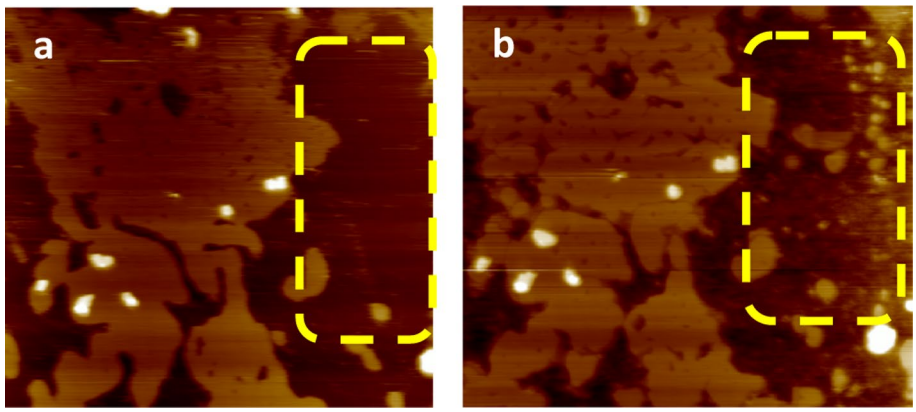

Fig. 5 Interaction of Bz-Arg-NHC_{10} with DPPC supported bilayers. AFM images (5 µm × 5 µm) taken **a** before the interaction and **b** 16 min after the injection of 50 µM Bz-Arg-NHC_{10}. Deposited material can be observed from the changes in the dashed zone

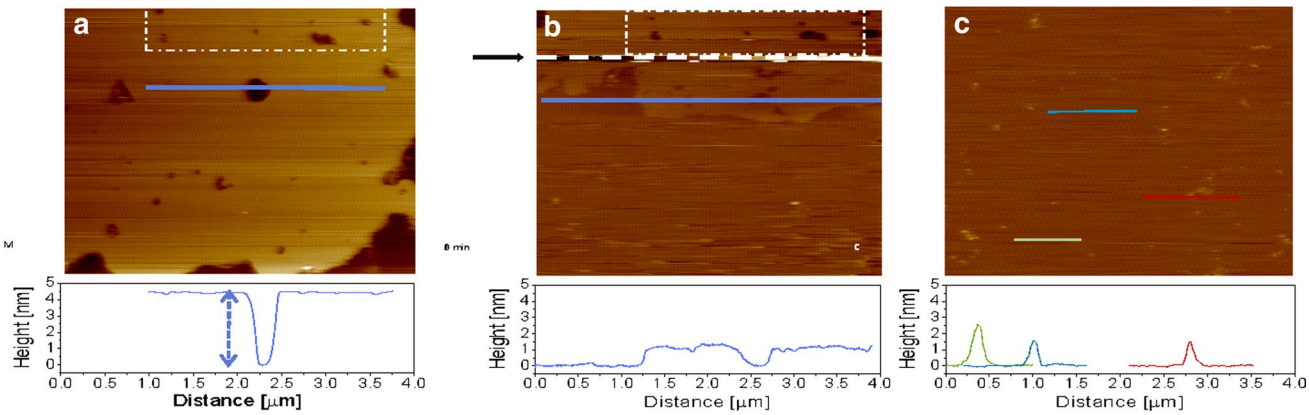

Fig. 6 AFM images of 100 µM Bz-Arg-NHC_{10} interaction with DPPC supported bilayers. **a** 4 µm × 4 µm image taken before the interaction with Bz-Arg-NHC_{10}, **b** injection of 100 µM Bz-Arg-NHC_{10} (arrow and black dotted line) and **c** subsequent scan at $t = 6$ min. Cross-sections shown below correspond to the full blue lines in the images. The white dotted rectangles in **a**, **b** show the conserved area between scans

The incubation of DPPC bilayers with the surfactant at a concentration two times greater than that used for the previous observations induced dramatic alterations of the bilayer (Fig. 6a, b). Indeed, after the addition of 100 µM Bz-Arg-NHC_{10}, the DPPC bilayer was completely removed leaving only patches of adsorbed material ranging 1.1–2.5 nm in mean height (Fig. 6c).

Surface plasmon resonance (SPR)

SPR constitutes a powerful biosensing technique for monitoring biomolecular interactions in real-time without labeling requirements. Biosensor experiments involve immobilizing one reactant on a surface and monitoring its interaction with a second component in solution through changes in the reflectivity of the Au sensor platform (Rich and Myszka 2000). Using SPR spectroscopy, we tested the binding and lipid solubilization capacity of Bz-Arg-NHC_{10} on DPPC supported lipid bilayers onto the surface of a sensor chip (Daza Millone et al. 2018). DPPC vesicles were injected in a step-way manner in order to reach different surface coverage and the surfactant was injected at concentrations 50, 100 and 500 µM (Fig. 7a).

When 500 µM of the surfactant was injected on sensors with a surface coverage higher than 29%, a net binding increase was detected, evidenced as an increment in the SPR signal, as shown in Fig. 7b. Similar results were obtained with lower (50 and 100 µM) surfactant concentrations. In contrast, a different profile was observed when 500 µM Bz-Arg-NHC_{10} was injected on sensor chips with 13% of lipid coverage. In this case, after surfactant injection, a drop of the signal below the baseline was observed, revealing the lipid removal from the bilayer. These results can be correlated with the AFM experiments performed at a surfactant concentration of 100 µM, in which the solubilization of the model biomembrane is observed (Fig. 6b).

In summary, the SPR response corresponds to both the adsorption of the surfactant which produces a disorganization of the DPPC bilayer and the release of lipid-detergent mixed micelles when the bilayers are saturated

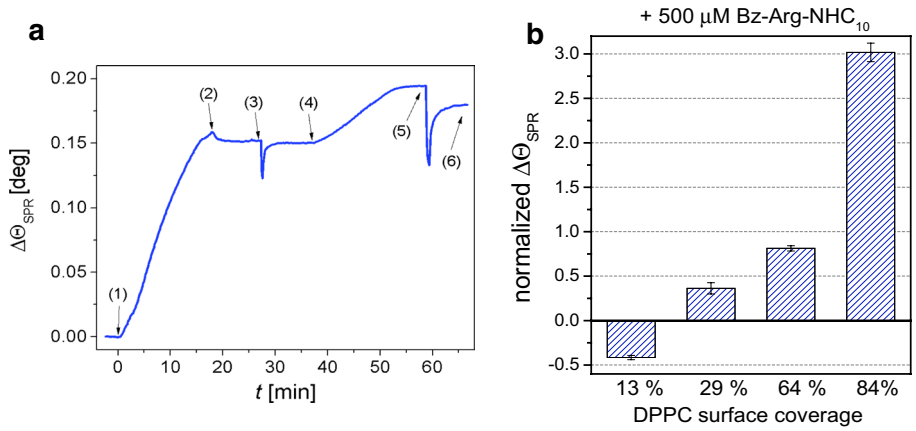

Fig. 7 SPR measurements of Bz-Arg-NHC_{10} binding to DPPC supported bilayers. **a** Interaction of 100 μM surfactant with ~ 40% DPPC surface coverage: (1) DPPC vesicle injection, (2) end of injection, (3) buffer washing step, (4) surfactant injection, (5) buffer washing step, and (6) final SPR signal showing a net increment. **b** Normalized changes in SPR angle—difference in values between (4) and (6) referred to lipid amount between (1) and (3)—for the interaction of 500 μM Bz-Arg-NHC_{10} with increasing DPPC surface coverage

by surfactant. These micelles can be re-deposited on the surface as shown in AFM images (Fig. 5b).

Discussion

A great effort has been made to design and synthesize a large variety of arginine-based surfactants with differences in the number of the cationic charges, the chemical structure of the head group, the number, length, and bonding positions of hydrophobic chains and the molecule's symmetry. In this paper, the interaction between Bz-Arg-NHC_{10} and lipid monolayers, liposomes and supported lipid bilayers has been studied with the aim of assessing the relationship between the chemical structure of the head group, in particular the presence of the benzoyl moiety, and the perturbation of membranes. Finally, these results were correlated with the antimicrobial activity of this surfactant.

The hydrophilic/hydrophobic balance of Bz-Arg-NHC_{10} due to the presence of benzoyl moiety attached to the head group lead to an effective insertion of the surfactant into the lipid bilayer. This property not only allowed the interaction of the surfactant with the membrane, but also increased the tendency to self-aggregate in solution, which is reflected in the low CMC value.

It was observed among different families of monocatenary arginine-based surfactants that the CMC values have a strong reliance on the alkyl chain length: the more hydrophobic the molecule (i.e., longer alkyl chain), the lower the CMC value. On the contrary, it is not clear whether the nature of the head group has an influence in the CMC and γ_{CMC} (Pinazo et al. 2019). Indeed, in terms of adsorption and surface-active properties, Bz-Arg-NHC_{10} has a much lower CMC value (from 5 to 150 times) than other arginine-based compounds—such as N^{α}-decyl-Arg-methyl ester (CAM) or Arg-*N*-decylamide (ACA)—(Pinazo et al. 2019). This could be attributed to the molecule's higher hydrophobicity due to the presence of the benzoyl group, which increases its tendency to self-aggregate. In this concern, Perinelli and coworkers reported the effect of the addition of a benzyl group on the CMC of quaternary ammonium leucine-based surfactants with the same alkyl chain length that Bz-Arg-NHC_{10} (Perinelli et al. 2019). They found that the substitution of the methyl group with a benzyl one exerts a double effect by increasing the hydrophobicity and the steric hindrance of the ammonium quaternary polar head, thereby reducing the CMC values.

Surfactants' micellization is influenced by the presence of salts in the medium: in general, CMC values of ionic surfactants become lower as the concentration of salts in the medium increases. The magnitude of this phenomenon depends on several factors, such as the ionic strength of the medium and the nature of the surfactant's counterion. The decrease of the CMC values would be a consequence of the reduction of the electrostatic repulsion forces among the head groups, due to an electrostatic shielding effect exerted by the ions present in the medium, and the increase of the interactions among the hydrophobic tails. Hence, an increment in the number of surfactant monomers per micelle is also observed (Helenius et al. 1979).

It is known that a change in the molecule's polarity has a direct influence in its ability to adsorb onto the surface as well as its insertion within a lipid membrane. To elucidate the disruption mechanism of the membrane organization, different approaches were adopted in this paper. Within this context, DSC experiments proved that Bz-Arg-NHC_{10} is slightly efficient in fluidizing DPPC bilayers within the concentration range tested. A similar trend was observed

for other arginine-based surfactants as N^{α}-lauroyl-Arg-methyl ester (LAM), which showed a small effect in the ΔT_m and $\Delta T_{1/2}$ values up to a 5 mol% concentration, but it became significant as the surfactant proportion increased (Castillo et al. 2004).

Moreover, Bz-Arg-NHC_{10} molecules demonstrated to be able to insert themselves within the membrane, as it arises from the monolayer insertion experiments. By these means, the value of π_c obtained was 59.6 mN m^{-1} for Bz-Arg-NHC_{10} in DPPC monolayers. This value by far exceeds the average π assigned to the lipid packing in cell membranes (30 mN m^{-1}), suggesting that Bz-Arg-NHC_{10} has the ability to penetrate into biological membranes even at high lipid packing densities (Marsh 1996). Interestingly, the net variation of the maximum π (π_{max}), can arise from the detergent-like behavior of this compound that once incorporated into the lipid film may reach a surface concentration high enough to induce the lipid removal from the monolayer to the aqueous subphase by the formation of mixed micelles (Nitenberg et al. 2018). Supporting this hypothesis, SPR responses and AFM images showed a similar trend, suggesting both the adsorption of the surfactant's molecules—which produces a disorganization of the DPPC bilayer—and the release of lipid-detergent mixed micelles once the bilayers become saturated with the surfactant's monomers. These micelles can be re-deposited on the surface, as shown in AFM images.

In all the experiments detailed in this paper, the surfactant concentration responsible for the effects observed was above its CMC value. The fact that the effects on the lipid bilayers were proportional to the surfactant concentration suggests that not only the monomers triggered membrane disruption through their insertion and mixed micelles releasing after saturation, but that also the surfactant aggregates can extract lipids via collision with the membrane.

Remarkably, all the results presented here are in concordance with the proposed hemolytic mechanism for Bz-Arg-NHC_{10} (Fait et al. 2017). In this regard, surfactants often exhibit a dual behavior: besides the hemolytic effect, they can also protect erythrocytes against hypotonic lysis. This protective effect is often observed at surfactant concentrations below the corresponding CMC value. However, our previous published work demonstrated that Bz-Arg-NHC_n display both hemolytic and protective activity above this parameter (Fait et al. 2018). Moreover, Joondan and coworkers proved a similar trend for the hemolytic activity of aromatic amino acid-based surfactants, evidencing the crucial role of the surfactants' aggregates in the disruption of the membrane structure (Joondan et al. 2016, 2017; Fait et al. 2018).

The discussion presented up to this point allows us to explain the results obtained in regard to the antimicrobial activity observed for Bz-Arg-NHC_{10}. As opposed to the results obtained for other arginine-based surfactants analogous to our compound, Bz-Arg-NHC_{10} showed a broad-spectrum antimicrobial activity: e.g., its MIC value for *E. coli* is 0.45 mM, whereas ACA and CAM proved to be ineffective against this microorganism. This can be explained based on the structural differences between these two compounds and Bz-Arg-NHC_{10}, which could result in different interactions with the bacterial cell surface and the microbial membrane. Furthermore, these interactions could be influenced not only by the chemical structure of the surfactant molecule, but also by the composition of bacterial cell envelopes themselves. It is also remarkable that Bz-Arg-NHC_{10} showed antimicrobial activity against both gram-positive and gram-negative bacterial strains in almost the same extent, a fact that is opposed to the behavior observed for other arginine-based surfactants, which were more effective against gram-positive bacteria (Fait et al. 2015). This behavior can be attributed to the presence of the benzoyl group, which increases the hydrophobic character of the surfactant, improving the surfactant molecules' ability to penetrate through the outer membrane of the gram-negative bacteria. Interestingly, this trend was also noticed by Perinelli and coworkers, who found that the *N*-benzyl group present in the cationic amino acid-based surfactants they studied enhanced the antimicrobial effect of this kind of compounds (Perinelli et al. 2019). The underlying principle for this behavior was addressed to the increase of the hydrophobicity of the molecule, especially for the derivative with a ten-carbon alkyl moiety.

Another feature of relevance concerns to MIC values reported in the literature for other amino acid derived surfactants, which are generally below the corresponding CMC value in water. This may lead to the assumption that the surfactant monomers and not its aggregates are the entities responsible for the antimicrobial activity. However, this was not observed for Bz-Arg-NHC_{10}, since the MIC values registered for this compound are above its CMC.

Finally, we consider that further studies using lipid membranes containing anionic lipids and PE are necessary to confirm whether the proposed mechanisms of interaction with red blood cells and DPPC membranes can be extrapolated to the bacterial membrane, explaining the antimicrobial mechanism of our surfactants.

Acknowledgements Financial support of MINCyT (PICT 2013-00647, PICT 2018-1651 and PICT 2016-0679), CONICET (PUE 22920170100100CO, PIP 2015-2017 1120201501 00671CO) and UNLP (11X-828 and 11/X861) is acknowledged. MH was awarded CONICET fellowship. MEF, RFV, SM, MADM and SRM are members of the CONICET Researcher Career. MEV and LB belong to the CICPBA Researcher Career.

Compliance with ethical standards

Conflict of interest The authors declare that they have no conflict of interest. This article does not contain any studies with human or animal subjects performed by the any of the authors.

References

Castillo JA, Pinazo A, Carilla J et al (2004) Interaction of antimicrobial arginine-based cationic surfactants with liposomes and lipid monolayers. Langmuir 20:3379–3387. https://doi.org/10.1021/la036452h

Castillo JA, Infante MR, Manresa À et al (2006) Chemoenzymatic synthesis and antimicrobial and haemolytic activities of amphiphilic bis(phenylacetylarginine) derivatives. ChemMedChem 1:1091–1098. https://doi.org/10.1002/cmdc.200600148

Colomer A, Pinazo A, Manresa MA et al (2011) Cationic surfactants derived from lysine: effects of their structure and charge type on antimicrobial and hemolytic activities. J Med Chem 54:989–1002. https://doi.org/10.1021/jm101315k

Colomer A, Perez L, Pons R et al (2013) Mixed monolayer of DPPC and lysine-based cationic surfactants: an investigation into the antimicrobial activity. Langmuir 29:7912–7921. https://doi.org/10.1021/la401092j

Daza Millone MA, Vázquez RF, Maté SM, Vela ME (2018) Phase-segregated membrane model assessed by a combined SPR-AFM Approach. Colloids Surf B Biointerfaces 172:423–429. https://doi.org/10.1016/j.colsurfb.2018.08.066

Epand R, Epand R (2009) Lipid domains in bacterial membranes and the action of antimicrobial agents. Biochim Biophys Acta Biomembr 1788:289–294. https://doi.org/10.1016/j.bbamem.2008.08.023

Fait ME, Garrote GL, Clapés P et al (2015) Biocatalytic synthesis, antimicrobial properties and toxicity studies of arginine derivative surfactants. Amino Acids 47:1465–1477. https://doi.org/10.1007/s00726-015-1979-0

Fait ME, Hermet M, Comelles F et al (2017) Microvesicle release and micellar attack as the alternative mechanisms involved in the red-blood-cell-membrane solubilization induced by arginine-based surfactants. RSC Adv. https://doi.org/10.1039/c7ra03640j

Fait ME, Hermet M, Vazquez R et al (2018) Volume expansion of erythrocytes is not the only mechanism responsible for the protection by arginine-based surfactants against hypotonic hemolysis. Colloids Surf B Biointerfaces. https://doi.org/10.1016/j.colsurfb.2018.07.005

Fait M, Bakas L, Garrote G et al (2019) Cationic surfactants as antifungal agents. Appl Microbiol Biotechnol 103:97–112. https://doi.org/10.1007/s00253-018-9467-6

Helenius A, McCaslin DR, Fries E, Tanford C (1979) Properties of detergents. Methods in enzymology. Academic Press, New York, pp 734–749

Infante MR, Molinero J, Erra P et al (1985) A comparative study on surface active and antimicrobial properties of some N^{α}-lauroyl-L^{α}, ωDibasic aminoacids derivatives. Fette Seifen Anstrichm 87:309–313. https://doi.org/10.1002/lipi.19850870805

Infante M, Pinazo A, Seguer J (1997) Non-conventional surfactants from amino acids and glycolipids: structure, preparation and properties. Colloids Surf A Physicochem Eng Asp 123–124:49–70. https://doi.org/10.1016/S0927-7757(96)03793-4

Inoue T, Iwanaga T, Fukushima K, Shimozawa R (1988) Biphasic effect of alkyltrimethylammonium bromides on gel-to-liquid-crystalline phase transition temperature of dilauroylphosphatidic acid (DLPA) vesicle membrane. Chem Lett 17:277–280. https://doi.org/10.1246/cl.1988.277

Joondan N, Jhaumeer Laulloo S, Caumul P et al (2016) Synthesis, physicochemical properties and membrane interaction of novel quaternary ammonium surfactants derived from L-tyrosine and L-DOPA in relation to their antimicrobial, hemolytic activities and in vitro cytotoxicity. Colloids Surf A Physicochem Eng Asp 511:120–134. https://doi.org/10.1016/j.colsurfa.2016.09.050

Joondan N, Jhaumeer Laulloo S, Caumul P (2017) Amino acids: building blocks for the synthesis of greener amphiphiles. J Dispers Sci Technol 39:1550–1564. https://doi.org/10.1080/01932691.2017.1421085

Lima L, Giannotti M, Redondo-Morata L et al (2013) Morphological and nanomechanical behavior of supported lipid bilayers on addition of cationic surfactants. Langmuir 29:9352–9361. https://doi.org/10.1021/la400067n

Lind T, Skoda M, Cárdenas M (2019) Formation and characterization of supported lipid bilayers composed of phosphatidylethanolamine and phosphatidylglycerol by vesicle fusion, a simple but relevant model for bacterial membranes. ACS Omega 4:10687–10694. https://doi.org/10.1021/acsomega.9b01075

Marsh D (1996) Lateral pressure in membranes. Biochim Biophys Acta Rev Biomembr 1286:183–223. https://doi.org/10.1016/S0304-4157(96)00009-3

Morán C, Clapés P, Comelles F et al (2001) Chemical structure/property relationship in single-chain arginine surfactants. Langmuir 17:5071–5075. https://doi.org/10.1021/la010375d

Morán MC, Pinazo A, Pérez L et al (2004) "Green" amino acid-based surfactants. Green Chem 6:233–240. https://doi.org/10.1039/b400293h

Morandat S, El Kirat K (2007) Solubilization of supported lipid membranes by octyl glucoside observed by time-lapse atomic force microscopy. Colloids Surf B Biointerfaces 55:179–184. https://doi.org/10.1016/j.colsurfb.2006.11.039

Müller D, Janovjak H, Lehto T et al (2002) Observing structure, function and assembly of single proteins by AFM. Prog Biophys Mol Biol 79:1–43

Nitenberg M, Bénarouche A, Maniti O et al (2018) The potent effect of mycolactone on lipid membranes. PLoS Pathog 14:1–30. https://doi.org/10.1371/journal.ppat.1006814

Perinelli DR, Petrelli D, Vitali LA et al (2019) Quaternary ammonium leucine-based surfactants: the effect of a benzyl group on physicochemical properties and antimicrobial activity. Pharmaceutics 11:287. https://doi.org/10.3390/pharmaceutics11060287

Pinazo A, Pons R, Pérez L, Infante MR (2011) Amino acids as raw material for biocompatible surfactants. Ind Eng Chem Res 50:4805–4817. https://doi.org/10.1021/ie1014348

Pinazo A, Pérez L, Morán M, Pons R (2019) Arginine-based surfactants: synthesis, aggregation properties, and applications, 2nd edn. Elsevier Inc., Amsterdam

Rich R, Myszka D (2000) Advances in surface plasmon resonance biosensor analysis. Curr Opin Biotechnol 11:54–61. https://doi.org/10.1016/S0958-1669(99)00054-3

Rosen M (2004) Surfactants and interfacial phenomena. Wiley, Hoboken

Tripathy DB, Mishra A, Clark J, Farmer T (2018) Synthesis, chemistry, physicochemical properties and industrial applications of amino acid surfactants: a review. Comptes Rendus Chim 21:112–130. https://doi.org/10.1016/j.crci.2017.11.005

Publisher's Note Springer Nature remains neutral with regard to jurisdictional claims in published maps and institutional affiliations.